Volume 19 | Number 11 | 21 March 2017 | Pages 7433–8122

PCCP

Physical Chemistry Chemical Physics

rsc.li/pccp

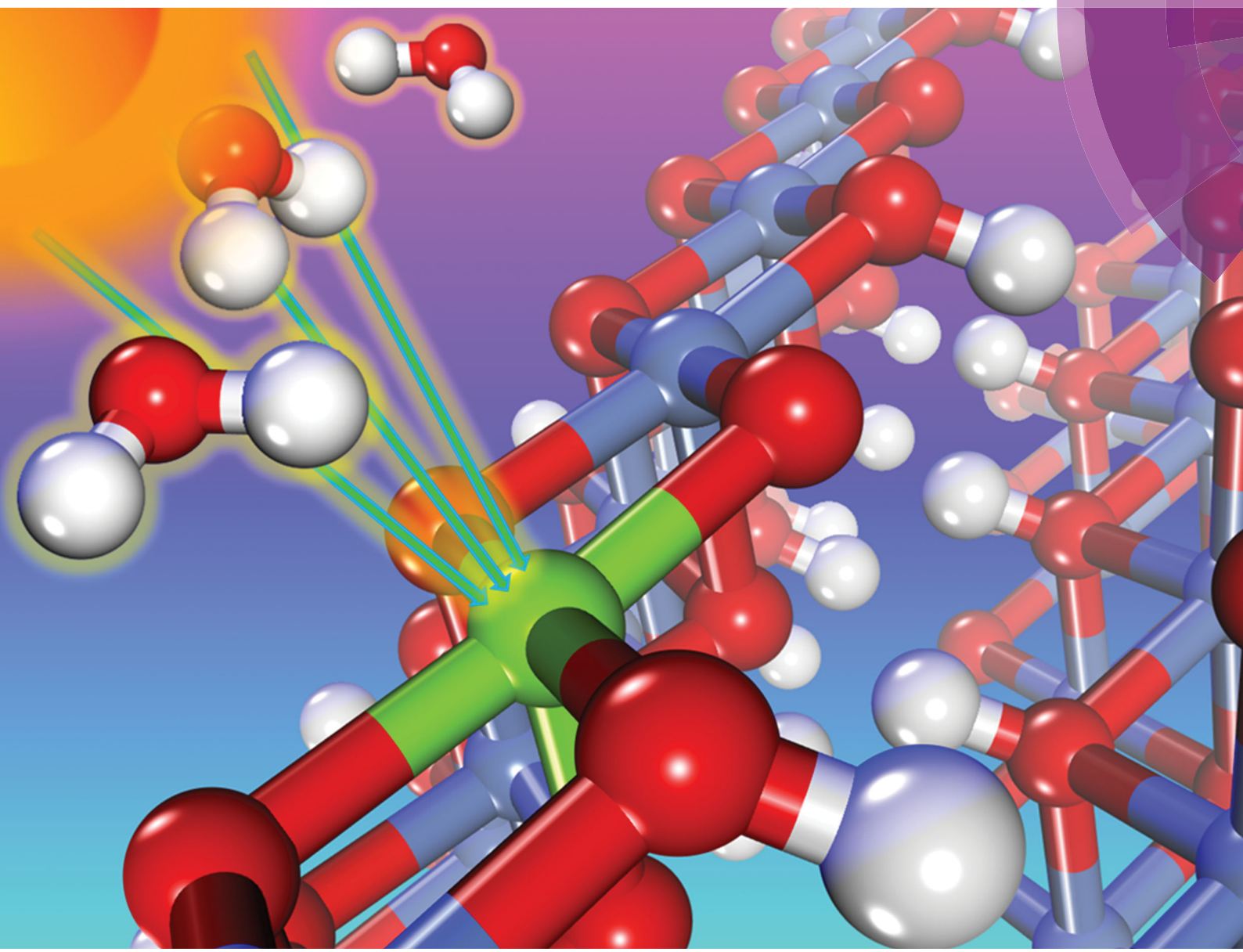

ISSN 1463-9076

ROYAL SOCIETY OF CHEMISTRY

PAPER

Vicky Fidelsky and Maytal Caspary Toroker

The secret behind the success of doping nickel oxyhydroxide with iron

PCCP

PAPER

View Article Online
View Journal | View Issue

Published on 08 February 2017. Downloaded by Technion - Israel Institute of Technology on 19/07/2017 10:02:36.

Cite this: *Phys. Chem. Chem. Phys.*, 2017, **19**, 7491

The secret behind the success of doping nickel oxyhydroxide with iron†

Vicky Fidelsky[a] and Maytal Caspary Toroker*[b]

Received 16th December 2016,
Accepted 8th February 2017

DOI: 10.1039/c6cp08590c

rsc.li/pccp

Discovering better catalysts for water splitting is the holy grail of the renewable energy field. One of the most successful water oxidation catalysts is nickel oxyhydroxide (NiOOH), which is chemically active only as a result of doping with Fe. In order to shed light on how Fe improves efficiency, we perform Density Functional Theory +U (DFT+U) calculations of water oxidation reaction intermediates of Fe substitutional doped NiOOH. The results are analyzed while considering the presence of vacancies that we use as probes to test the effect of adding charge to the surface. We find that the smaller electronegativity of the Fe dopant relative to Ni allows the dopant to have several possible oxidation states with less energy penalty. As a result, the presence of vacancies which alters local oxidation states does not affect the low overpotential of Fe-doped NiOOH. We conclude that the secret to the success of doping NiOOH with iron is the ability of iron to easily change oxidation states, which is critical during the chemical reaction of water oxidation.

1. Introduction

The constant usage of fossil fuels for generating electricity is harming our environment. One of the alternatives for generating energy is electrochemical water splitting, where catalytic materials are used to cleave water into oxygen gas and clean hydrogen fuel.[1–3] In this context, there have been many studies attempting to understand what controls water splitting catalysis with the aim of developing better materials for splitting water.[4,5]

NiOOH is one of the best catalysts for the oxygen evolution reaction (OER) under alkaline conditions.[6] However, recently there has been evidence that the high efficiency of NiOOH is due to Fe contaminants.[7,8] As a result, the interest in Fe-doped NiOOH is growing, where experimental studies have analyzed the performance of this catalyst.[9–11] In addition, several electrochemical devices have adapted NiOOH into their architectures, such as covering Fe_2O_3 with an NiOOH overlayer.[12]

Furthermore, a number of theoretical studies have been devoted to modeling the catalytic activity of NiOOH.[13,14] In agreement with experiments, the calculated overpotential for water oxidation with Fe-doping was found to be smaller than that in the pure case.[15,16] According to these calculations, there is a general agreement that the active site responsible for this activity is the iron dopant.[16] However, aside from reporting the calculated overpotential, there has been no explanation for why Fe improves catalytic efficiency.

In our own previous theoretical work, we have obtained a typical "volcano" curve which shows that the binding energy of reactants is optimal for Fe doping of NiOOH in comparison to other first-row transition metal dopants.[17] Furthermore, we found that late transition metals, including Fe, Co, Cu, and Zn, should be more catalytically active than early transition metals, such as Ti, due to the larger bonding ionicity of the latter.[18] However, these studies do not pin-point the reason for why Fe is exceptional.

Since the Fe atom can acquire several oxidation states in various systems and this property has been demonstrated to be useful for catalysis in other systems,[19] we chose to investigate how Fe changes in the complex environment of NiOOH. The NiOOH system is challenging since Ni itself acquires several oxidation states and since the surface charging state can change during operating conditions.

In order to shed light on the origin of the success of doping NiOOH with Fe, we perform Density Functional Theory +U (DFT+U) calculations of water oxidation on the NiOOH surface, while it is doped with Fe. We note that in this work we focus on the β phase of NiOOH which does not include the option of a penetrating electrolyte in order to simplify the analysis and since we wish to compare to previous theoretical work that studied this phase.[15,17] We also consider H and OH vacancies which is instructive for modeling the reactivity of doped NiOOH since they show how well the material can donate or accept

[a] *The Nancy and Stephen Grand Technion Energy Program, Technion – Israel Institute of Technology, Haifa 3200003, Israel*
[b] *Department of Materials Science and Engineering, Technion – Israel Institute of Technology, Haifa 3200003, Israel. E-mail: maytalc@tx.technion.ac.il; Tel: +972 4 8294298*

† Electronic supplementary information (ESI) available: Further details on free energy calculations, atomic magnetic moments, and unit cells used for the surfaces are provided. See DOI: 10.1039/c6cp08590c

Published on 08 February 2017. Downloaded by Technion - Israel Institute of Technology on 19/07/2017 10:02:36.

electrons, respectively. We find that the low overpotential of Fe-doped NiOOH does not change as a result of vacancies that affect local oxidation states, indicating that Fe can obtain several possible oxidation states in NiOOH with a small energy penalty.

2. Methods and calculation details

The VASP program was used to perform spin-polarized Density Functional Theory (DFT) calculations.[20,21] The Perdew–Burke–Ernzerhof (PBE)[22] functional with the DFT+U formalism from the study of Duradev *et al.*[23] was used. The effective U–J term was taken to be 5.5 eV and 3.3 eV for Ni and Fe, respectively, as previously done for modeling catalysis of doped NiOOH.[15,24–27] In our previous work, we found that the free energies of water oxidation catalysis for doped β-NiOOH are dependent on the choice of U values,[17] as presented for a variety of systems in ref. 28, and that only these values reproduce reliable results in comparison with experiments. Projected-augmented wave (PAW) potentials replaced the core electrons of Ni 1s2s2p3s3p, Fe 1s2s2p3s3p, and O 1s.[29,30]

The unit cell of β-NiOOH[15,31–34] was cleaved at the $(0\bar{1}5)$ plane for two reasons. First, this facet was interpreted to be chemically active.[15] Second, this surface was studied in previous literature and we wanted to compare it with previous results.[15] Hence, the same slab sizes were built as in ref. 15 for comparison.[26] The dependence of the slab size for various electronic properties, such as band edge positions and reaction free energies, was tested in our previous studies on β-NiOOH$(0\bar{1}5)$.[17,26] Doping was considered at a substitutional site of the active site since previous models as well as some experimental evidence suggest that the dopant is the active site.[15,16] Vacancies were added to each reaction intermediate slab model at the site closest to the active site in order to have the maximal effect of the vacancy (see Fig. 1). We considered H vacancies since these are expected to appear at large bias and pH. We also modeled OH vacancies since these are expected to provide an additional understanding of the effect of charging the surface with an excess electron.[35] Overall, we use both defects as probes to test how the material reactivity changes in response to the addition of charge carriers. The energy cutoff of 600 eV and the k-point Gamma-centered grid of $2 \times 2 \times 1$ were converged to within <1 meV. The ion positions were converged until the force components on all the ions were less than 0.03 eV Å^{-1}. The optimized unit cells are given in the ESI.†

We considered the following four-step mechanism that has been studied in ref. 15, for comparison, and under alkaline conditions carries the following form:

$$A + h^+ + OH^- \rightarrow B + H_2O \quad (1)$$

$$B + h^+ + OH^- \rightarrow C \quad (2)$$

$$C + h^+ + OH^- \rightarrow D + H_2O \quad (3)$$

$$D + h^+ + OH^- \rightarrow A + O_2 \quad (4)$$

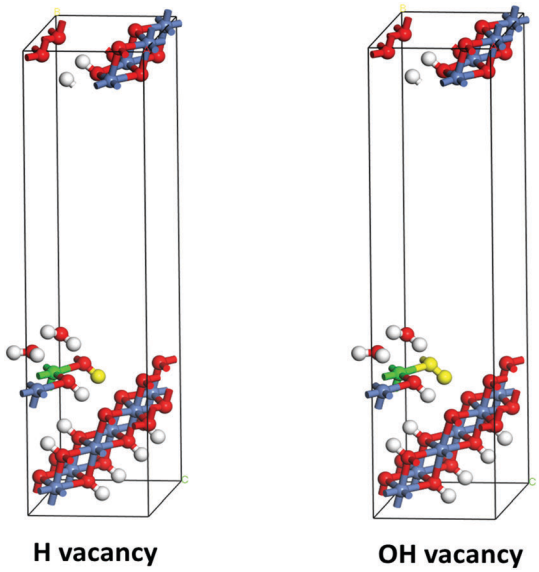

Fig. 1 Surface unit cells showing the location of H and OH vacancies as well as the Fe dopant at the active site. Red, blue, and white spheres represent the oxygen, nickel, and hydrogen atoms, respectively. Yellow and green spheres represent the vacancy and the Fe dopant, respectively.

where intermediate "A" is a slab with a monolayer of adsorbed water molecules and intermediate "B" has one hydroxyl group termination. Intermediate "C" has a monolayer of adsorbed water molecules and an additional oxygen atom penetrating the surface. Intermediate "D" has one hydroxyl group termination and an additional oxygen atom penetrating the surface. The slab models for each intermediate are shown in Fig. 2. The free energy for the reactions was calculated by subtracting the total energy of reactants and products and adding the previously reported Zero Point Energy (ZPE) corrections and entropic contributions of pure β-NiOOH since these additions were shown to be stable with variations in composition.[15,36] The free energies were calculated at 1 Volts and pH = 14 which are the known operating conditions for the OER with NiOOH. The applied voltage is considered by adding a constant energy $-eU$ to the free energy of each reaction. The pH is considered by adding the term $-k_B T \cdot \ln 10 \cdot \text{pH}$, where k_B is the Boltzmann constant and T is the temperature, 298.15 K. The overpotential is defined as the voltage that needs to be added to the calculated electrochemical potential so that all reaction free energies are negative.

The calculated results were analyzed in terms of atomic oxidation states. The oxidation states of Ni atoms were inferred from the atomic magnetizations. The +2, +3, and +4 oxidation states can be related to two, one, and no singly occupied orbitals, respectively. These oxidation states roughly correspond to the calculated magnetizations of ~1.7, 1.2, and 0.2 Bohr magneton, respectively. Similarly, the oxidation states of Fe atoms are +2, +3, +4, +5, and +6 which are related to four, five, four, three, and two singly occupied states in the high spin state. These oxidation states roughly correspond to the calculated magnetizations of ~3.4, 4.0, 3.4, 2.8, and 2.1 Bohr magneton for an electronic configuration of $t_{2g}^4 e_g^2$, $t_{2g}^3 e_g^2$, $t_{2g}^3 e_g^1$, t_{2g}^3, and t_{2g}^2, respectively.

This journal is © the Owner Societies 2017

Published on 08 February 2017. Downloaded by Technion - Israel Institute of Technology on 19/07/2017 10:02:36.

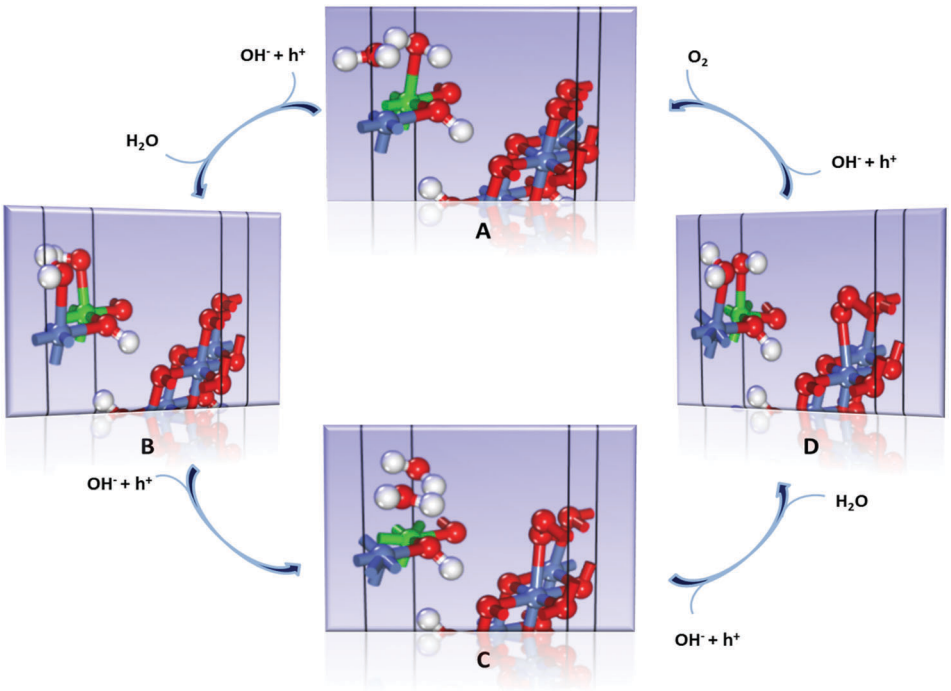

Fig. 2 The water oxidation reaction for Fe-doped NiOOH with a H deficiency. The geometries are fully optimized.

Note that these are tentative assignments, since there is some uncertainty in the oxidation states due to several possible spin states that may exist (high spin and low spin states). In fact, magnetization of 2.2 could also correspond to the lower spin states: t_{2g}^4 and $t_{2g}^5e_g^1$, *i.e.* oxidation states +4 and +2, respectively. Hence, the oxidation states are assigned based on comparison between different reaction intermediates with several stoichiometries and by analogy with the magnetization in other oxide materials.[37]

3. Results

In this section, we present free energy calculations of the water oxidation reaction for Fe-doped and non-stoichiometric NiOOH. First, we compare the free energies for water oxidation on pure NiOOH with those of Fe-doped NiOOH. Next, we consider the effect of H and OH vacancies on the doped case and find that they have little effect.

The overpotential for water oxidation with NiOOH reduces significantly upon Fe-doping at the active site (see Table 1). The Fe dopant is located at the active site at a substitutional site, since previous theoretical and experimental studies showed that this is the preferred and chemically active location.[16] The free energies of the first two reactions are the same (~ -0.4 eV) for the case of Fe-doping. This is ideal for catalysis: the spread of the free energies equally upon several reaction steps reduces the overpotential.[38] Similar free energies for the first deprotonation reactions indicate that Fe can change between oxidation states with a similar energy requirement. Specifically, as seen in Fig. 3, for example, the oxidation state of Fe changes from +4 to +5 during the first deprotonation reaction (see the table of atomic magnetization in the ESI†). During this reaction of deprotonating the adsorbed water molecule, the magnetic moment on Ni atoms does not change, while iron is only affected. The oxidation state of the active site is expected to be the same in intermediates A and C that have an adsorbed water molecule (and in intermediates B and D that have an adsorbed hydroxyl group), but the remarkable result shown in Fig. 3 demonstrates that Fe can have a variety of stable oxidation states. Therefore, Fe is an effective dopant for NiOOH.

Table 1 Free energies and overpotentials for pure and Fe-doped NiOOH at pH = 14 and V = 1 Volts. The values for pure NiOOH are adapted from ref. 39

Reaction	Pure NiOOH	Fe-Doped NiOOH
A to B	−0.11	−0.41
B to C	−0.71	−0.36
C to D	−0.40	−0.56
D to A	−1.58	−1.48
Overpotential	**0.61**	**0.36**

In contrast to Fe-doped NiOOH, the energy required for the first step is higher for pure NiOOH (−0.11 eV in Table 1). The first step of increasing the oxidation state is easier for Fe relative to Ni since Fe is a less electronegative transition metal. Hence, Fe can exist in several oxidation states. We note that our results are in excellent agreement with previous theoretical studies for the doped case with no added vacancies[15,36] (free energies without potential and pH corrections are given in the ESI†).

The efficiency of OER largely depends on the ability of the active site transition metal to change its oxidation state. In the first reaction step, a transition metal at the active site is oxidized and increases in oxidation state, while in the second reaction

Published on 08 February 2017. Downloaded by Technion - Israel Institute of Technology on 19/07/2017 10:02:36.

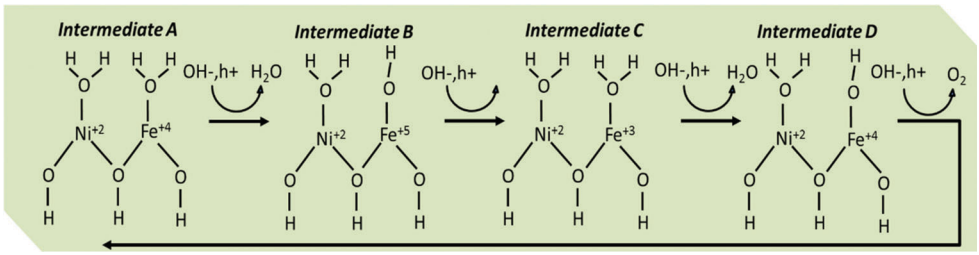

Fig. 3 Sketch of the changes in atomic formal charges during the water oxidation reaction for the Fe-doped NiOOH material. Only the topmost layer is presented for clarity.

step the transition metal reduces. During the first deprotonation reaction, the oxidation state of Ni changes from +3 to +4 for pure NiOOH[39] and the oxidation state of Fe changes from +4 to +5 for Fe-doped NiOOH. In the second reaction where water is adsorbed again on the active site, the oxidation state of Ni and Fe changes to +3 for both pure and Fe-doped NiOOH, respectively. In pure NiOOH, although Ni can exist in a few oxidation states, the preferred one is +3, which is the oxidation state for the majority of Ni atoms in NiOOH,[15,39] in agreement with the average experimentally observed oxidation state.[40] Hence, for pure NiOOH, the free energy of the first reaction step is larger than the second (in Table 1, for pure NiOOH, the free energy for the first reaction, −0.11 eV, is larger than the free energy of the second reaction, −0.71 eV). In contrast, for Fe-doped NiOOH, the free energy of the first and second reactions is similar due to the ability of Fe to change between several oxidation states.

Since the ability to change the oxidation state is a key ingredient, we add vacancies as probes since they change the local oxidation states. The change in the oxidation state may arise either due to the deprotonation chemical reactions or due to the addition of vacancies. Vacancies induce excess charge: H and OH vacancies contribute an excess hole and electron, respectively.

The effect of vacancies on the water oxidation overpotential with Fe-doped NiOOH is small. We chose the locations of the vacancies to be in proximity to the active site so that they can give the maximal effect. As seen in Table 2, for Fe doping, the addition of either an H or OH vacancy does not change significantly the free energy of the reaction with the highest overpotential. For Fe-doped NiOOH, the second reaction denoted "B to C" has a free energy of around ∼(−0.4)–(−0.2) eV with or without vacancies. Some variations are also seen in other reactions, but these are not affecting the overpotential.

The small effect of vacancies on the overpotential of Fe-doped NiOOH can be visualized by observing the cumulative free energies.

Table 2 Free energies and overpotentials for Fe-doped NiOOH with or without H or OH vacancies at pH = 14 and V = 1 Volts

Reaction	Pure NiOOH	Fe-Doped NiOOH	Fe-Doped NiOOH with H vacancy	Fe-Doped NiOOH with OH vacancy
A to B	−0.11	−0.41	−0.81	−0.64
B to C	−0.71	−0.36	−0.39	−0.18
C to D	−0.40	−0.56	−0.62	−0.97
D to A	−1.58	−1.48	−0.98	−1.01
Overpotential	**0.61**	**0.36**	**0.33**	**0.54**

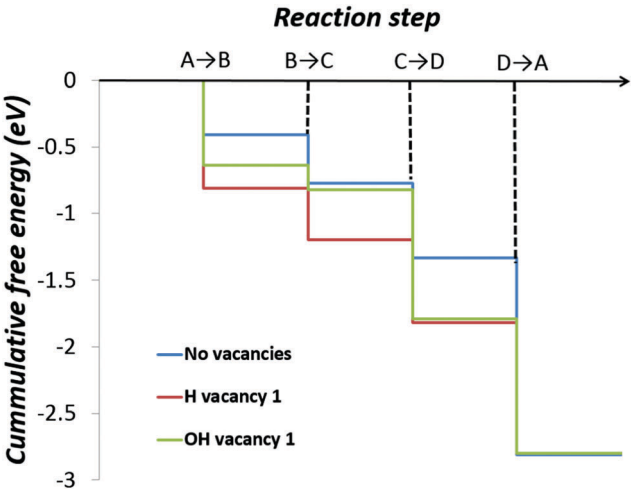

Fig. 4 Cumulative free energies for water oxidation reaction for Fe-doped NiOOH in the pure, H vacancy, and OH vacancy case.

As seen in Fig. 4, the steps representing the cumulative free energies have some similarities. The general distribution of free energies among the reaction steps is generally the same in many cases, especially the rise from B to C. There is a slight increase in the overpotential when an OH vacancy is present for Fe-doped NiOOH, since this type of vacancy tends to decrease the energy required for the first deprotonation (and increase the free energy for the second deprotonation) due to the excess charge that neutralizes and stabilizes intermediate B. We note that the presence of H vacancies is more probable than OH vacancies under realistic operating conditions of large bias and pH.

In our previous paper,[39] we observed that for non-stoichiometric and undoped NiOOH, the formal charge of oxygen near a H vacancy changed from −2 to −1 and the formal charge on Ni as the active site was +2.5 when there was an OH vacancy. Each one of these vacancies destabilized the surface, reduced the free energy of reaction A to B, and resulted in a significant decrease in overpotential, in agreement with a recent experiment that demonstrates enhanced OER activity upon deprotonation.[41]

However, we find that in the Fe doped case, the addition of the H vacancy does not change the oxidation state of the oxygen atom close to the vacancy. Instead, Ni has a higher +3 oxidation state (Fig. 5). In the presence of a H vacancy, the oxidation state of Fe is +4 in intermediates A and C, and turns into +5 in

 This journal is © the Owner Societies 2017

Published on 08 February 2017. Downloaded by Technion - Israel Institute of Technology on 19/07/2017 10:02:36.

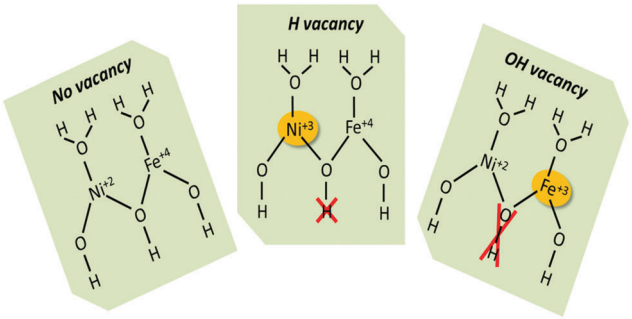

Fig. 5 Sketch of the changes in atomic formal charges upon vacancy formation for intermediate A in the water oxidation reaction with Fe-doped NiOOH. Left: Intermediate A with no vacancy, center: intermediate A with a H vacancy, and right: intermediate A with an OH vacancy.

intermediates B and D after elementary deprotonation reactions. Furthermore, the addition of an OH vacancy changes the oxidation state of Fe from +4 to +3 in intermediate A (Fig. 5). In the presence of an OH vacancy, the oxidation state of Fe is +3 in intermediates A and C, and turns into +4 in intermediates B and D after elementary deprotonation reactions. These changes have little effect on the overpotential. Similar to the pure case, the vacancies destabilize intermediate A and reduce the free energy required for reaction A to B. As we explain below, the charging effect of the vacancies has little effect on the free energy required for reaction B to C, which determines the overpotential for Fe-doped NiOOH.

An instructive criterion to analyze surface reactivity is to correlate the type of excess charge generated by the vacancy with the free energies. In our previous work on the surface reactivity of Fe_2O_3,[35,37,42] we found that defects that generate excess holes such as iron vacancies increase the free energy of early deprotonation steps. Since the Fe_2O_3 surface is already charged with holes as a result of Fe vacancies, taking more electrons out during deprotonation is difficult from the beginning. Similarly, defects that generate excess electrons such as n-type dopants increase the free energies of later reaction steps. Hence, we found a rule correlating the type and the amount of charge with the free energy changes.

Our rule is useful for the pure and Fe-doped NiOOH system. Intermediate A is stable for both the pure and doped case since Fe doping does not change the sum of overall oxidation states; Fe is not an n-type or a p-type dopant.[18] Without any vacancy, the neutral intermediate is A. The H vacancy introduces a hole to the surface, and earlier intermediate D is neutral and stable. Hence, reactions that involve intermediate D are affected: the free energy for reaction D to A increases, while the free energy for reaction C to D is reduced as a result of H vacancy addition. In addition, since intermediate A is now not neutral and hence less stable, reactions that involve intermediate A are also affected: the free energy for reaction A to B decreases, while the free energy for reaction D to A again increases. As seen in Table 2, for Fe-doped NiOOH as an example, the free energies of reactions A to B, D to A, and C to D are −0.41, −1.48, and −0.56 eV before H addition and −0.81, −0.98, and −0.62 eV after H addition.

An important consequence of Fe doping is that a H vacancy does not change the relative stability of intermediates B and C significantly, since Fe at the active site can more readily change oxidation states (as seen in Table 2, the free energy is −0.4 eV with or without a H vacancy). In contrast, for pure NiOOH, the stability of intermediate B is affected due to the H addition that alters an oxygen's oxidation state.[39] Hence, the free energy of reaction B to C as well as the overpotential is not influenced by a H vacancy for Fe-doped NiOOH.

In contrast, with an OH vacancy there is an excess electron and intermediate B is more stable. Reactions that involve intermediate B are affected: the free energy for reaction A to B decreases, while the free energy for reaction B to C increases as a result of OH vacancy addition. Similarly, since intermediate A is now not neutral and hence less stable, reactions that involve intermediate A are also affected: the free energy for reaction A to B decreases, while the free energy for reaction D to A again increases. This explains the small rise in the overpotential due to OH addition for Fe-doped NiOOH.

4. Conclusions

The effect of Fe-doping NiOOH on the OER activity was investigated by analyzing the changes in atomic oxidation states. We conclude that Fe is a successful dopant since it can possess several oxidation states. Specifically, a similar free energy is needed for the transition of Fe(III) to Fe(V) and Fe(V) to Fe(III) in the first two deprotonation steps of the OER for Fe-doped NiOOH. In contrast, pure NiOOH requires a large free energy for the first deprotonation for the transition of Ni(III) to Ni(IV). Ni itself has three oxidation states in NiOOH, but Ni(III) is most common and any deviation from this state is less favorable.

We added vacancies to the models as a "test bed" for evaluating how well the surface catalyzes in the presence of excess charge; an H vacancy introduces an excess hole, while an OH vacancy induces an excess electron. We used vacancies to introduce excess charge since a key factor determining OER reactivity is the ability of the surface to accept charge during electrochemical operation.

In order to rationalize our results, we used a rule we derived earlier that correlates overpotential with surface charging.[35,37,42] The addition of vacancies charges and destabilizes intermediate A, and decreases the free energy of reaction (1) in both the doped and undoped cases. Since Fe is able to switch back and forth between the oxidation states in the first two reactions, in the presence of vacancies reaction (1) has a smaller free energy, but reaction (2) still has the same free energy. Hence, the overpotential does not change significantly in the presence of vacancies for Fe-doped NiOOH.

We note that efficient heterogeneous catalysis depends not only on low free energies of the reaction, but also on good charge transport abilities of the catalyst. The electronic conductivity of the catalysts is important for driving charge carriers to the surface for participating in a chemical reaction. It has been hypothesized[43] that Fe-doped NiOOH is a good catalyst

Published on 08 February 2017. Downloaded by Technion - Israel Institute of Technology on 19/07/2017 10:02:36.

since it has both high catalytic performance and high electronic conductivity since it may have a band-like mechanism for charge transport. In our previous work,[44] we demonstrated that nickel hydroxide indeed has delocalized states even after Fe-doping. Here we provide direct proof that Fe has good catalytic performance in the environment of NiOOH. This study contributes to unlocking the puzzle behind the success of Fe-doped NiOOH.

Acknowledgements

This research was supported by the Nancy and Stephen Grand Technion Energy Program, the I-CORE Program of the Planning and Budgeting Committee, and The Israel Science Foundation (Grant No. 152/11) as well as SPIRA Fund for Applied Research in the Field of Energy. This work was supported by the post LinkSCEEM-2 project, funded by the European Commission under the 7th Framework Programme through Capacities Research Infrastructure, INFRA-2010-1.2.3 Virtual Research Communities, Combination of Collaborative Project and Coordination and Support Actions (CP-CSA) under grant agreement no RI-261600. V. F. acknowledges the scholarship provided by the Jacob Isler Foundation.

References

1 T. Hisatomi, J. Kubota and K. Domen, Recent Advances in Semiconductors for Photocatalytic and Photoelectrochemical Water Splitting, *Chem. Soc. Rev.*, 2014, **43**, 7520–7535.
2 M. G. Walter, E. L. Warren, J. R. McKone, S. W. Boettcher, Q. Mi, E. A. Santori and N. S. Lewis, Solar Water Splitting Cells, *Chem. Rev.*, 2010, **110**, 6446–6473.
3 H. Dotan, N. Mathews, T. Hisatomi, M. Grätzel and A. Rothschild, On the Solar to Hydrogen Conversion Efficiency of Photoelectrodes for Water Splitting, *J. Phys. Chem. Lett.*, 2014, **5**, 3330–3334.
4 S. Chen, S. S. Thind and A. Chen, Nanostructured Materials for Water Splitting – State of the Art and Future Needs: A Mini-Review, *Electrochem. Commun.*, 2016, **63**, 10–17.
5 N. Serpone, A. V. Emeline, V. K. Ryabchuk, V. N. Kuznetsov, Y. M. Artem'ev and S. Horikoshi, Why Do Hydrogen and Oxygen Yields from Semiconductor-Based Photocatalyzed Water Splitting Remain Disappointingly Low? Intrinsic and Extrinsic Factors Impacting Surface Redox Reactions, *ACS Energy Lett.*, 2016, 931–948.
6 F. Dionigi and P. Strasser, NiFe-Based (Oxy)Hydroxide Catalysts for Oxygen Evolution Reaction in Non-Acidic Electrolytes, *Adv. Energy Mater.*, 2016, 1600621.
7 L. J. Enman, M. S. Burke, A. S. Batchellor and S. W. Boettcher, Effects of Intentionally Incorporated Metal Cations on the Oxygen Evolution Electrocatalytic Activity of Nickel (Oxy)-Hydroxide in Alkaline Media, *ACS Catal.*, 2016, **6**, 2416–2423.
8 L. Trotochaud, S. L. Young, J. K. Ranney and S. W. Boettcher, Nickel–Iron Oxyhydroxide Oxygen-Evolution Electrocatalysts: The Role of Intentional and Incidental Iron Incorporation, *J. Am. Chem. Soc.*, 2014, **136**, 6744–6753.
9 L. Cai, J. Zhao, H. Li, J. Park, I. S. Cho, H. S. Han and X. Zheng, One-Step Hydrothermal Deposition of Ni:Feooh onto Photoanodes for Enhanced Water Oxidation, *ACS Energy Lett.*, 2016, **1**, 624–632.
10 S. Klaus, Y. Cai, M. W. Louie, L. Trotochaud and A. T. Bell, Effects of Fe Electrolyte Impurities on Ni(OH)2/NiOOH Structure and Oxygen Evolution Activity, *J. Phys. Chem. C*, 2015, **119**, 7243–7254.
11 F. Dionigi, T. Reier, Z. Pawolek, M. Gliech and P. Strasser, Design Criteria, Operating Conditions, and Nickel–Iron Hydroxide Catalyst Materials for Selective Seawater Electrolysis, *ChemSusChem*, 2016, **9**, 962–972.
12 F. Malara, A. Minguzzi, M. Marelli, S. Morandi, R. Psaro, V. Dal Santo and A. Naldoni, α-Fe_2O_3/NiOOH: An Effective Heterostructure for Photoelectrochemical Water Oxidation, *ACS Catal.*, 2015, **5**, 5292–5300.
13 V. Fidelsky, V. Butera, J. Zaffran and M. C. Toroker, Three Fundamental Questions on One of Our Best Water Oxidation Catalysts: A Critical Perspective, *Theor. Chem. Acc.*, 2016, **135**, 162.
14 O. Diaz-Morales, I. Ledezma-Yanez, M. T. M. Koper and F. Calle-Vallejo, Guidelines for the Rational Design of Ni-Based Double Hydroxide Electrocatalysts for the Oxygen Evolution Reaction, *ACS Catal.*, 2015, **5**, 5380–5387.
15 Y.-F. Li and A. Selloni, Mechanism and Activity of Water Oxidation on Selected Surfaces of Pure and Fe-Doped NiOx, *ACS Catal.*, 2014, **4**, 1148–1153.
16 D. Friebel, *et al.*, Identification of Highly Active Fe Sites in (Ni,Fe)OOH for Electrocatalytic Water Splitting, *J. Am. Chem. Soc.*, 2015, **137**, 1305–1313.
17 J. Zaffran and M. C. Toroker, Designing Efficient Doped NiOOH Catalysts for Water Splitting with First Principles Calculations, *ChemistrySelect*, 2016, **1**, 911–916.
18 J. Zaffran and M. C. Toroker, Metal–Oxygen Bond Ionicity as an Efficient Descriptor for Doped NiOOH Photocatalytic Activity, *ChemPhysChem*, 2016, **17**, 1630–1636.
19 J. L. Fillol, Z. Codolà, I. Garcia-Bosch, L. Gómez, J. J. Pla and M. Costas, Efficient Water Oxidation Catalysts Based on Readily Available Iron Coordination Complexes, *Nat. Chem.*, 2011, **3**, 807–813.
20 G. Kresse and J. Hafner, Ab Initio Molecular Dynamics for Liquid Metals, *Phys. Rev. B: Condens. Matter Mater. Phys.*, 1993, **47**, 558–561.
21 G. Kresse and J. Furthmüller, Efficiency of Ab-Initio Total Energy Calculations for Metals and Semiconductors Using a Plane-Wave Basis Set, *Comput. Mater. Sci.*, 1996, **6**, 15–50.
22 J. P. Perdew, K. Burke and M. Ernzerhof, Generalized Gradient Approximation Made Simple, *Phys. Rev. Lett.*, 1996, **77**, 3865–3868.
23 S. L. Dudarev, G. A. Botton, S. Y. Savrasov, C. J. Humphreys and A. P. Sutton, Electron-Energy-Loss Spectra and the Structural Stability of Nickel Oxide: an Lsda+U Study, *Phys. Rev. B: Condens. Matter Mater. Phys.*, 1998, **57**, 1505–1509.
24 Y.-F. Li and A. Selloni, Mosaic Texture and Double C-Axis Periodicity of β-NiOOH: Insights from First-Principles and

 This journal is © the Owner Societies 2017

Published on 08 February 2017. Downloaded by Technion - Israel Institute of Technology on 19/07/2017 10:02:36.

Genetic Algorithm Calculations, *J. Phys. Chem. Lett.*, 2014, **5**, 3981–3985.

25 A. J. Tkalych, K. Yu and E. A. Carter, Structural and Electronic Features of β-Ni(OH)2 and β-NiOOH from First Principles, *J. Phys. Chem. C*, 2015, **119**, 24315–24322.

26 V. Fidelsky and M. Caspary Toroker, Engineering Band Edge Positions of Nickel Oxyhydroxide through Facet Selection, *J. Phys. Chem. C*, 2016, **120**, 8104–8108.

27 J. Zaffran and M. Caspary Toroker, Benchmarking Density Functional Theory Based Methods to Model NiOOH Material Properties: Hubbard and van der Waals Corrections Vs Hybrid Functionals, *J. Chem. Theory Comput.*, 2016, **12**, 3807.

28 M. Capdevila-Cortada, Z. Łodziana and N. López, Performance of DFT+U Approaches in the Study of Catalytic Materials, *ACS Catal.*, 2016, **6**, 8370–8379.

29 P. E. Blöchl, Projector Augmented-Wave Method, *Phys. Rev. B: Condens. Matter Mater. Phys.*, 1994, **50**, 17953–17979.

30 G. Kresse and D. Joubert, From Ultrasoft Pseudopotentials to the Projector Augmented-Wave Method, *Phys. Rev. B: Condens. Matter Mater. Phys.*, 1999, **59**, 1758–1775.

31 M. Casas-Cabanas, J. Canales-Vázquez, J. Rodríguez-Carvajal and M. R. Palacín, Deciphering the Structural Transformations During Nickel Oxyhydroxide Electrode Operation, *J. Am. Chem. Soc.*, 2007, **129**, 5840–5842.

32 P. Oliva, J. Leonardi, J. F. Laurent, C. Delmas, J. J. Braconnier, M. Figlarz, F. Fievet and A. D. Guibert, *J. Power Sources*, 1982, **8**, 229–255.

33 R. G. Delaplane, J. A. Ibers, J. R. Ferraro and J. J. Rush, Diffraction and Spectroscopic Studies of the Cobaltic Acid System HCoC2–DCoO2, *J. Chem. Phys.*, 1969, **50**, 1920–1927.

34 J. Chen and A. Selloni, First Principles Study of Cobalt (Hydr)Oxides under Electrochemical Conditions, *J. Phys. Chem. C*, 2013, **117**, 20002–20006.

35 M. C. Toroker, Theoretical Insights into the Mechanism of Water Oxidation on Nonstoichiometric and Titanium-Doped Fe2O3(0001), *J. Phys. Chem. C*, 2014, **118**, 23162–23167.

36 F. Costanzo, Effect of Doping β-NiOOH with Co on the Catalytic Oxidation of Water: DFT+U Calculations, *Phys. Chem. Chem. Phys.*, 2016, **18**, 7490–7501.

37 O. Neufeld and M. C. Toroker, Platinum-Doped α-Fe_2O_3 for Enhanced Water Splitting Efficiency: A DFT+U Study, *J. Phys. Chem. C*, 2015, **119**, 5836–5847.

38 J. K. Norskov, T. Bligaard, J. Rossmeisl and C. H. Christensen, Towards the Computational Design of Solid Catalysts, *Nat. Chem.*, 2009, **1**, 37–46.

39 V. Fidelsky and M. Caspary Toroker, Enhanced Water Oxidation Catalysis of Nickel Oxyhydroxide through the Addition of Vacancies, *J. Phys. Chem. C*, 2016, **120**, 25405.

40 R. Barnard, C. F. Randell and F. L. Tye, Studies Concerning Charged Nickel Hydroxide Electrodes I. Measurement of Reversible Potentials, *J. Appl. Electrochem.*, 1980, **10**, 109–125.

41 O. Diaz-Morales, D. Ferrus-Suspedra and M. T. M. Koper, The Importance of Nickel Oxyhydroxide Deprotonation on Its Activity Towards Electrochemical Water Oxidation, *Chem. Sci.*, 2016, **7**, 2639–2645.

42 N. Yatom and M. Toroker, Hazardous Doping for Photo-Electrochemical Conversion: The Case of Nb-Doped Fe2O3 from First Principles, *Molecules*, 2015, **20**, 19668.

43 M. S. Burke, S. Zou, L. J. Enman, J. E. Kellon, C. A. Gabor, E. Pledger and S. W. Boettcher, Revised Oxygen Evolution Reaction Activity Trends for First-Row Transition-Metal (Oxy)Hydroxides in Alkaline Media, *J. Phys. Chem. Lett.*, 2015, **6**, 3737–3742.

44 V. Butera and M. Caspary Toroker, Electronic Properties of Pure and Fe-Doped β-Ni(OH)2: New Insights Using Density Functional Theory with a Cluster Approach, *J. Phys. Chem. C*, 2016, **120**, 12344–12350.